frontiers in
MICROBIOLOGY

ORIGINAL RESEARCH ARTICLE
published: 18 June 2012
doi: 10.3389/fmicb.2012.00224

Genetic and biochemical identification of a novel single-stranded DNA-binding complex in *Haloferax volcanii*

Amy Stroud[1], Susan Liddell[2] and Thorsten Allers[1]*

[1] School of Biology, Queen's Medical Centre, University of Nottingham, Nottingham, UK
[2] Division of Animal Sciences, University of Nottingham, Loughborough, UK

Edited by:
Zvi Kelman, University of Maryland, USA

Reviewed by:
Jocelyne DiRuggiero, The Johns Hopkins University, USA
Stuart MacNeill, University of St Andrews, UK

***Correspondence:**
Thorsten Allers, School of Biology, Queen's Medical Centre, University of Nottingham, Nottingham NG7 2UH, UK.
e-mail: thorsten.allers@nottingham.ac.uk

Single-stranded DNA (ssDNA)-binding proteins play an essential role in DNA replication and repair. They use oligonucleotide/oligosaccharide-binding (OB)-folds, a five-stranded β-sheet coiled into a closed barrel, to bind to ssDNA thereby protecting and stabilizing the DNA. In eukaryotes the ssDNA-binding protein (SSB) is known as replication protein A (RPA) and consists of three distinct subunits that function as a heterotrimer. The bacterial homolog is termed SSB and functions as a homotetramer. In the archaeon *Haloferax volcanii* there are three genes encoding homologs of RPA. Two of the *rpa* genes (*rpa1* and *rpa3*) exist in operons with a novel gene specific to Euryarchaeota; this gene encodes a protein that we have termed RPA-associated protein (*rpap*). The *rpap* genes encode proteins belonging to COG3390 group and feature OB-folds, suggesting that they might cooperate with RPA in binding to ssDNA. Our genetic analysis showed that *rpa1* and *rpa3* deletion mutants have differing phenotypes; only Δ*rpa3* strains are hypersensitive to DNA damaging agents. Deletion of the *rpa3*-associated gene *rpap3* led to similar levels of DNA damage sensitivity, as did deletion of the *rpa3* operon, suggesting that RPA3 and RPAP3 function in the same pathway. Protein pull-downs involving recombinant hexahistidine-tagged RPAs showed that RPA3 co-purifies with RPAP3, and RPA1 co-purifies with RPAP1. This indicates that the RPAs interact only with their respective associated proteins; this was corroborated by the inability to construct *rpa1 rpap3* and *rpa3 rpap1* double mutants. This is the first report investigating the individual function of the archaeal COG3390 RPA-associated proteins (RPAPs). We have shown genetically and biochemically that the RPAPs interact with their respective RPAs, and have uncovered a novel single-stranded DNA-binding complex that is unique to Euryarchaeota.

Keywords: archaea, *Haloferax volcanii*, RPA single-strand DNA-binding protein, COG3390 RPA-associated protein, DNA repair, protein overexpression, Cdc48d

INTRODUCTION

Genomic DNA must be unwound in order to be replicated or repaired, leaving it vulnerable to nuclease and chemical attack as well as open to the possibility of forming secondary structures. Binding of the single-stranded DNA (ssDNA)-binding proteins (SSB) RPA and SSB prevents any of these events from occurring (Lu et al., 2009). The SSB is denominated SSB in bacteria and replication protein A (RPA) in eukaryotes; they bind to ssDNA with high affinity and to dsDNA and RNA with low affinity (Wobbe et al., 1987; Wold et al., 1989; Kim et al., 1992). They play a vital organizational role in the central genome maintenance of the cell, providing docking platforms for a wide range of enzymes to gain access to genomic substrates (Lu and Keck, 2008). The bacteriophage T4 gene 32 monomer was the first SSB to be identified (Alberts and Frey, 1970). RPA was first identified as an essential protein for DNA replication in the eukaryotic simian virus (SV40; Wobbe et al., 1987) by stimulating the T antigen-mediated unwinding of the SV40 origin of replication (Kenny et al., 1989). RPA and SSB have now been established as essential proteins for DNA metabolism including DNA replication, recombination, and repair in all domains of life (Wobbe et al., 1987; Heyer et al., 1990; Coverley et al., 1991, 1992; Moore et al., 1991; Wold, 1997). The basic architecture of RPA and SSB is based on the oligonucleotide/oligosaccharide-binding (OB)-fold, a five-stranded β-sheet coiled into a closed barrel, but the number of OB-folds present varies from species to species (Bochkarev and Bochkareva, 2004; Fanning et al., 2006).

Unlike in bacteria and eukaryotes, the architecture of SSBs present in archaea is not uniform. There is wide diversity of SSBs in the two main archaeal phyla, Euryarchaea, and Crenarchaea. Crenarchaea possess SSBs similar to those of bacteria, consisting of a single subunit with one OB-fold and an acidic C-terminus tail (Rolfsmeier and Haseltine, 2010). Euryarchaea have RPA-like proteins that show homology with the eukaryotic RPA, but from species to species the architecture of euryarchaeal RPAs varies dramatically from a single polypeptide RPA to an RPA made up of several subunits. Each of these RPAs can contain up to four OB-folds as well as a zinc finger motif (Rolfsmeier and Haseltine, 2010).

Pyrococcus furiosus RPA consists of three subunits RPA41, 14, and 32, denominated RPA1, 2, and 3, respectively, which form a heterotrimer as seen in eukaryotes. Strand exchange and immunoprecipitation assays have shown that *P. furiosus* heterotrimeric RPA stimulates strand exchange, and interacts with the clamp loader RFC and both DNA polymerases B and D (Komori and Ishino, 2001). The heterotrimeric complex seen in *P. furiosus* is also found in *P. abyssi* and *P. horikoshii*. However, in other archaeal species the *rpa* genes have undergone lineage-specific duplications, resulting in differing numbers of SSBs with diverse structures. Unlike the RPA complex found in *Pyrococcus* spp., or eukaryotic RPA, these do not form trimeric complexes (Robbins et al., 2004).

Methanosarcina acetivorans possesses three RPA subunits, MacRPA1, 2, and 3, which are unlikely to form a heterotrimeric complex as seen in *P. furiosus* and in eukaryotes. MacRPA1 contains four DNA-binding domains (DBD) containing OB-folds, MacRPA2 and 3 both have two OB-fold containing DBDs. Each of the three MacRPAs can function as SSBs, and are able to stimulate primer extension by *M. acetivorans* DNA polymerase BI (Robbins et al., 2004, 2005). This demonstrates an element of redundancy between the three MacRPAs, and suggests that the heterotrimeric RPA structure observed in *P. furiosus* is the exception and not the rule. Lin et al. (2008) suggest that intramolecular recombination between RPA homologs may have led to the diversity of RPAs found in euryarchaea, which can function in different pathways or cellular processes.

A similar pattern of lineage-specific gene duplication is seen with the archaeal MCM helicase, where the number and type of MCM subunits that make up the hexameric helicase differ between archaeal species. The genes encoding the MCM subunits fall into distinct phylogenetic clades, but these do not correspond to specific subunits of eukaryotic MCM. Instead they have arisen through lineage-specific gene family expansion (Chia et al., 2010). Such gene duplication might allow different archaeal species to refine the structure and function of MCM (and potentially RPA) for differing conditions and specialized roles.

Sulfolobus solfataricus has a bacterial-like SSB consisting of a small 20 kDa peptide containing one OB-fold and an acidic C-terminus tail (Haseltine and Kowalczykowski, 2002; Rolfsmeier and Haseltine, 2010). The *S. solfataricus* SSB quaternary structure is similar to that of *E. coli* SSB, however the primary structure of the OB-fold shows greater homology to that of the eukaryotic RPA70 DNA-binding domain B (DBDB). This suggests that crenarchaeal SSBs may be structurally similar to bacterial SSB but at a protein sequence level show homology to the eukaryotic RPA (Haseltine and Kowalczykowski, 2002; Kerr et al., 2003). In *S. solfataricus* there is an absence of DNA damage recognition proteins such as homologs of XPA or XPC to initiate NER. The ability of *S. solfataricus* SSB to specifically bind and melt damaged duplex DNA *in vitro* suggests SSB may play a role in the identification and binding of damaged DNA, followed by the subsequent recruitment of NER repair proteins (Cubeddu and White, 2005).

Haloferax volcanii encodes three RPA genes *rpa1*, *rpa2*, and *rpa3* (Hartman et al., 2010). Recent studies have shown RPA2 to be essential while RPA1 and RPA3 are not (Skowyra and MacNeill, 2012). Note that these authors used the nomenclature *rpaA1*, *A2*, *B1*, *B2*, *B3*, and *C* to refer to *rpa3*, *rpap3*, *rpa1*, *rpap1*, *rpe*, and *rpa2*, respectively, while we have chosen to maintain the official nomenclature as described in Table 4 of the *H. volcanii* genome paper (Hartman et al., 2010). Both *rpa1* and *rpa3* are in operons with other genes; *rpa1* is in an operon with genes encoding an OB-fold containing protein (hereby designated RPA-associated protein or RPAP) and a calcineurin-like phosphoesterase, while only one OB-fold rpa-associated protein (*rpap*) gene is present in the *rpa3* operon (**Figure 1**). The presence of an *rpap* gene in the same operon as *rpa* can be found in other euryarchaeota, including *Halobacterium marismortui*, *Halobacterium salinarum*, and *Natronomonas pharaonis*, as well as in *M. mazei* and *M. barkeri*. The *rpap* gene has been assigned to the cluster of orthologous groups (COG) 3390 (Berthon et al., 2008).

To examine if RPA1 and 3, as well as RPAP1 and RPAP3 play a role in DNA repair, as is true for both the bacterial SSB and eukaryotic RPA, DNA damage assays were performed using the single and operon deletion mutants. Cells with deletions of the *rpa1* and *rpa3* operons had previously been examined by Skowyra and MacNeill (2012). However, this is the first report investigating the individual function of the archaeal COG3390 RPAP. We show genetically and biochemically that the RPAPs interact with their respective RPAs, and have thereby uncovered a novel SSB complex that is unique to Euryarchaeota.

MATERIALS AND METHODS

All chemicals were from Sigma and restriction enzymes from New England Biolabs, unless stated otherwise. Standard molecular techniques were used (Sambrook and Russell, 2001).

STRAINS AND PLASMIDS

Haloferax volcanii strains (**Table 1**) were grown at 45°C on complete (Hv-YPC), casamino acids (Hv-Ca), or minimal (Hv-Min) agar, or in Hv-YPC or Hv-Ca broth as described previously. Isolation of genomic and plasmid DNA, as well as transformation of *H. volcanii* were carried out as described previously (Allers et al., 2004).

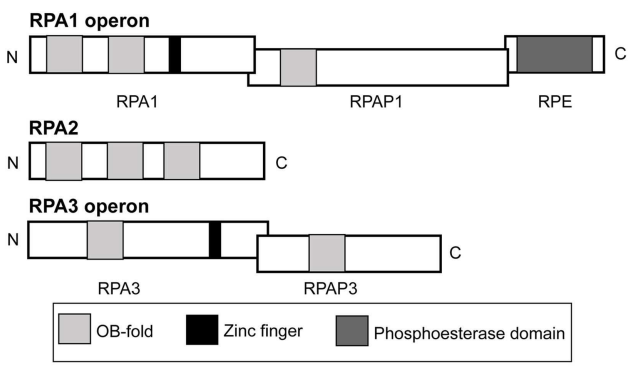

FIGURE 1 | Operon and domain structures of *H. volcanii* single-stranded DNA-binding proteins. Genes for RPA1 and RPA3 are in operons with genes for RPA-associated proteins, RPAP1 and RPAP3, respectively. The gene for RPA1 phosphoesterase (RPE) is present in the *rpa1* operon. Domains (not to scale) comprising OB-folds, zinc fingers and a phosphoesterase motif are shown.

Table 1 | *Haloferax volcanii* strains.

Strain	Relevant genotype*	Source or reference
DS2	Wild-type	Mullakhanbhai and Larsen (1975)
H195	Δ*pyrE2 bgaHa-Bb leuB-Ag1* Δ*trpA* Δ*hdrB*	Guy et al. (2006)
H1209	Δ*pyrE2* Δ*hdrB Nph-pitA* Δ*mrr*	Allers et al. (2010)
H1216	Δ*pyrE2 bgaHa-Bb leuB-Ag1* Δ*trpA* Δ*hdrB* Δ*rpap1*::*trpA*+	H195 pTA1170
H1217	Δ*pyrE2 bgaHa-Bb leuB-Ag1* Δ*trpA* Δ*hdrB* Δ*rpa1*::*trpA*+	H195 pTA1166
H1244	Δ*pyrE2 bgaHa-Bb leuB-Ag1* Δ*trpA* Δ*hdrB* Δ*rpa3*::*trpA*+	H195 pTA1174
H1246	Δ*pyrE2 bgaHa-Bb leuB-Ag1* Δ*trpA* Δ*hdrB* Δ*rpa1 operon*	H195 pTA1189
H1260	Δ*pyrE2* Δ*hdrB bgaHa-Bb* Δ*rpa3 operon*::*trpA*+ *leuB-Ag1* Δ*trpA*	H195 pTA1207
H1280	Δ*pyrE2 bgaHa-Bb leuB-Ag1* Δ*trpA* Δ*hdrB* Δ*rpap1*	H1216 pTA1217
H1281	Δ*pyrE2 bgaHa-Bb leuB-Ag1* Δ*trpA* Δ*hdrB* Δ*rpa1*	H1217 pTA1141
H1282	Δ*pyrE2 bgaHa-Bb leuB-Ag1* Δ*trpA* Δ*hdrB* Δ*rpa1 operon rpa3 operon*+::[Δ*rpa3 operon*::*trpA*+, *pyrE2*+]	H1246 pTA1207 pop-in
H1326	Δ*pyrE2 bgaHa-Bb leuB-Ag1* Δ*trpA* Δ*hdrB* Δ*rpap1 rpa3*+::[Δ*rpa3*::*trpA*+ *pyrE2*+]	H1280 pTA1174 pop-in
H1333	Δ*pyrE2* Δ*hdrB Nph-pitA* Δ*mrr Hsa-cdc48d*	H1209 pTA1240
H1390	Δ*pyrE2 bgaHa-Bb leuB-Ag1* Δ*trpA* Δ*hdrB* Δ*rpa1 operon rpa3 operon*+::[Δ*rpa3 operon*::*trpA*+, *pyrE2*+] <*rpa1* operon+*hdrB*+*pyr*E2>	H1282 pTA1265 pop-in
H1410	Δ*pyrE2 bgaHa-Bb leuB-Ag1* Δ*trpA* Δ*hdrB* Δ*rpap3*	H195 pTA1284
H1424	Δ*pyrE2* Δ*hdrB Nph-pitA* Δ*mrr cdc48d-Ct*	H1333 pTA1294
H1430	Δ*pyrE2* Δ*hdrB Nph-pitA* Δ*mrr cdc48d-Ct* <*p.tna*::*his tag*+*pyrE2*+ *hdrB*+>	H1424 pTA963
H1473	Δ*pyrE2 bgaHa-Bb leuB-Ag1* Δ*trpA* Δ*hdrB* Δ*rpa1 rpap3*+::[Δ*rpap3*::*trpA*+ *pyrE2*+]	H1281 pTA1284 pop-in
H1480	Δ*pyrE2* Δ*hdrB Nph-pitA* Δ*mrr cdc48d-Ct* <*p.tnaA*::*his tag-rpa3 rpap3 pyrE2*+ *hdrB*+>	H1424 pTA1280
H1481	Δ*pyrE2* Δ*hdrB Nph-pitA* Δ*mrr cdc48d-Ct* <*p.tnaA*::*rpa3 his tag-rpap3 pyrE2*+ *hdrB*+>	H1424 pTA1281
H1482	Δ*pyrE2* Δ*hdrB Nph-pitA* Δ*mrr cdc48d-Ct* <*p.tnaA*::*his tag-rpa1 rpap1 pyrE2*+ *hdrB*+>	H1424 pTA1326
H1483	Δ*pyrE2* Δ*hdrB Nph-pitA* Δ*mrr cdc48d-Ct* <*p.tnaA*::*rpa1 his tag-rpap1 pyrE2*+ *hdrB*+>	H1424 pTA1327

**Genes shown within <> are present on an episomal plasmid, genes shown within [] are present on an integrated plasmid (pop-in).*

CONSTRUCTION OF MUTANT STRAINS

Deletion mutants were constructed as described previously (Allers et al., 2004). Plasmids for gene deletion are shown in **Table 2**, and were generated by PCR using oligonucleotides shown in **Table 3**. Template DNA for the PCRs was isolated from genomic DNA.

CONSTRUCTION OF PROTEIN OVEREXPRESSION STRAINS

Protein overexpression strains were constructed by transformation with episomal overexpression plasmids as described previously (Allers et al., 2010). Plasmids for protein expression are shown in **Table 2**, and were generated by PCR using oligonucleotides shown in **Table 3**. Template DNA for the PCRs was isolated from genomic DNA.

UV IRRADIATION ASSAYS

UV irradiation assays were carried out as described previously (Delmas et al., 2009).

MITOMYCIN C ASSAYS

Mitomycin C (MMC) assays were carried out as described previously (Lestini et al., 2010).

PROTEIN OVEREXPRESSION AND PURIFICATION

Protein overexpression was carried out as described previously (Allers et al., 2010) with the following amendments: cultures were incubated at 45°C overnight to an OD_{650} of 0.5, when protein expression was induced by adding 3 mM Trp to the culture followed by incubation at 45°C, with shaking for a further 1 h until $OD_{650} \approx 0.7$.

PROTEIN PRECIPITATION

Deoxycholate was added to 0.015%, vortexed, and incubated for 10 min at room temperature. Trichloroacetic acid was added to 7.2% and incubated at room temperature for 5 min. Samples were centrifuged at 14,000 × *g* at room temperature for 8 min. Supernatant was removed and precipitated protein resuspended in 15 µl resuspension buffer (330 mM Tris-HCl pH 7.2, 2.6% SDS, 17 mM NaOH, 5% glycerol, 0.25 mg/ml bromophenol blue). Samples were heated for 10 min at 94°C and cooled on ice before loading onto an SDS-PAGE gel.

MASS SPECTROMETRY

Mass spectrometry of excised protein bands was carried out as described previously (Allers et al., 2010). Details of protein identification are given in the **Table A1** in Appendix.

RESULTS

RPA3 BUT NOT RPA1 FUNCTIONS IN DNA REPAIR

In eukaryotes, specifically *Saccharomyces cerevisiae*, all three RPA subunits have been shown to be essential for cell survival (Brill and Stillman, 1991). Work by Skowyra and MacNeill (2012) has shown that *H. volcanii rpa2* is essential, which is in agreement with our fruitless attempts to delete *rpa2* (data not shown). To examine if the other *rpa* genes of *H. volcanii* are also essential,

Table 2 | Plasmids.

Plasmid	Relevant properties	Source or reference
pBluescript II SK+	Standard cloning vector	Stratagene
pTA131	Integrative vector based on pBluescript II, with *pyr*E2 marker	Allers et al. (2004)
pTA409	Shuttle vector containing ampicillin, *pyrE2* and *hdrB* markers, and pHV1/4 replication origin	Delmas et al. (2009)
pTA884	pBluescript II with *H. volcanii* 5,038-bp *Eco*RI/*Not*I genomic fragment containing *rpa3* operon	This study
pTA898	pBluescript II with *H. volcanii* 7,335-bp *Eco*RI/*Not*I genomic fragment containing *rpa2*	This study
pTA937	pBluescript II with *H. volcanii* 8,565-bp *Bsp*EI genomic fragment containing *rpa1* operon	This study
pTA963	Overexpression vector with 6xHis-tag, *pyr*E2 and *hdrB* markers, and pHV2 origin	Allers et al. (2010)
pTA1141	pTA131 containing *rpa1* deletion construct inserted at *Kpn*I and *Xba*I sites, contains an internal *Nde*I site	This study
pTA1142	pTA131 containing *rpa3* deletion construct inserted at *Eco*RI and *Kpn*I sites, contains an internal *Nde*I site	This study
pTA1166	*rpa1* deletion construct pTA1141 with *trpA* marker, amplified from pTA298 introducing *Nde*I restriction sites to insert at internal *Nde*I restriction site in pTA1141	This study
pTA1170	Deletion construct of *rpap1* containing *trpA* marker from pTA298 inserted at *Eco*RI and *Kpn*I sites in pTA131	This study
pTA1174	*rpa3* deletion construct containing *trpA* marker from pTA1166 inserted at *Nde*I restriction site	This study
pTA1180	pTA131 with *cdc48d* deletion construct	Allers et al. (2010)
pTA1189	pTA131 with *rpa1* operon deletion construct inserted at restriction sites *Xba*I and *Eco*RI with an internal *Nde*I site	This study
pTA1196	*rpa3* operon deletion construct, using *Nde*I/*Eco*RI downstream fragment from pTA1282 (*rpap3* deletion construct) inserted at *Nde*I/*Eco*RI sites in pTA1142 (*rpa3* deletion construct), to replace the downstream fragment of the *rpa3* deletion construct	This study
pTA1207	Deletion construct of *rpa3* operon pTA1196 with insertion of the *trpA* marker from pTA1166 at internal *Nde*I site	This study
pTA1217	*RPAP1* deletion construct pTA1170 with upstream and *trpA* fragment replaced with the upstream fragment amplified from pTA937 by PCR, to introduce compatible *Sph*I sites, generating non-*trpA*-marked deletion construct	This study
pTA1218	pTA963 with *rpa3* inserted downstream of His-tag. *Ase*I inserted after *rpa3* stop codon to allow insertion of His-tagged *rpa3* upstream of His-tagged *rpap3* (*Ase*I is *Nde*I compatible)	This study
pTA1222	pTA963 with *rpa1* N-terminally His-tagged, has an *Ase*I site downstream of *rpa1* to allow insertion of *rpap1* (*Nde*I compatible)	This study
pTA1223	pTA963 overexpression vector with *rpap1* N-terminally His-tagged inserted at *Psi*I and *Bam*HI sites. *rpap1* was amplified by PCR from pTA937 introducing *Bsp*HI and *Bam*HI sites	This study
pTA1224	pTA963 with *rpap3* N-terminally His-tagged inserted at *Psi*I and *Eco*RI sites. *RPAP3* was amplified by PCR from pTA884 introducing *Bsp*HI and *Eco*RI sites	This study
pTA1240	Gene replacement construct with insertion of 896 bp *Hsa-cdc48d* gene (amplified from *H. salinarum* DNA) between upstream and downstream flanking regions of *H. volcanii cdc48d* deletion construct pTA1180	This study
pTA1265	pTA409 with insertion of *rpa1* operon from pTA937 at *Eco*RV site	This study
pTA1280	pTA1218 with *rpap3* amplified from pTA884 by PCR and inserted at *Bst*EII and *Eco*RI sites after the N-terminally His-tagged *rpa3*, maintaining reading frame	This study
pTA1281	pTA1224 with *rpa3* amplified from pTA884 by PCR and inserted upstream of N-terminally His-tagged *rpap3* at *Nde*I site	This study
pTA1282	*rpap3* deletion construct with upstream and downstream regions amplified from genomic clone pTA884, introducing external *Kpn*I and *Eco*RI sites, used to ligate into pTA131, and internal *Nde*I site	This study
pTA1284	*rpap3* deletion construct pTA1282 with *trpA* marker digested from pTA1166 using *Nde*I and inserted at *Nde*I site in pTA1282, generating *trpA*-marked *rpap3* deletion construct	This study
pTA1288	pBluescript II with *H. volcanii* 3,299-bp *Sal*I/*Bsp*HI genomic fragment containing *cdc48d* gene	This study
pTA1294	pTA131 with 2,247 bp *Hvo-cdc48d-Ct* gene replacement construct amplified from pTA1288: 1,797 bp *Eco*RI-*Nhe*I fragment with C-terminally truncated *cdc48d* plus upstream region, ligated to 485 bp *Nhe*I-*Kpn*I fragment with downstream region of *cdc48d*, inserted at *Eco*RI and *Kpn*I sites	This study
pTA1326	pTA1222 with *rpap1*, amplified from pTA937 introducing *Bst*EII and *Bam*HI sites, and inserted downstream of His-tagged *rpa1* at *Bst*EII and *Bam*HI sites	This study
pTA1327	pTA1223 with *rpa1* inserted upstream of His-tagged *rpap1* at *Nde*I site. *rpa1* was amplified from pTA937 introducing *Nde*I and *Ase*I (*Nde*I compatible) sites	This study

Table 3 | Oligonucleotides.

Oligonucleotide	Sequence (5′–3′)	Relevant properties	Use (plasmid generated)
Rpa1CF DS	GTTCGAGGTACCGTTCGGGGAGC	Δ*rpa1* external downstream primer, *Kpn*I site	pTA1141
Rpa1CR DS	AGGTGCGCATATGAGCGCCTCGC	Δ*rpa1* internal downstream primer, *Nde*I site	pTA1141
Rpa1 CR US	TACTACGTCTAGACGGACCTGTTCG	Δ*rpa1* external upstream primer, *Xba*I site	pTA1141
Rpa1 CF US	GGTCGAGTTCCATATGGTCGGGATTCGCC	Δ*rpa1* internal upstream primer, *Nde*I site	pTA1141
Rpa3KpnI F	GCCGGTGGTACCACAGCCTC	Δ*rpa3* external upstream primer, *Kpn*I site	pTA1142
Rpa3NdeIR	GCAAATCAGTCATATGCTACCTCGCC	Δ*rpa3* internal upstream primer, *Nde*I site	pTA1142
Rpa3EcoRIR	GACGGTGGAATTCGGCCGTCG	Δ*rpa3* external downstream primer, *Eco*RI site	pTA1142
Rpa3NdeI FC	GCGAGGTCGATGCATATGAGTTCCAACG	Δ*rpa3* internal downstream primer, *Nde*I site	pTA1142
trpANdeIF	CTCTGCACATATGTCGCTCGAAGACGC	*trpA* forward primer containing *Nde*I site	pTA1166
trpANdeIR	TGCATGCCATATGCGTTATGTGCG	*trpA* reverse primer containing *Nde*I	pTA1166
RPAP11kpnIus	CCGCGAGTGGTACCGCAAGCCCG	Δ*rpap1* external upstream primer, *Kpn*I site	pTA1170
RPAP11nsiIus	CGACGACCGGCGATGCATTCATGCGCGC	Δ*rpap1* internal upstream primer, *Nsi*I site	pTA1170
RPAP11sphIds	GCTGAAGGGCATGCGAGGCCGTGC	Δ*rpap1* internal downstream primer, *Sph*I site	pTA1170
RPAP11ecoRIds	CGGCGAGAGAATTCCCTGCCCGGG	Δ*rpap1* external downstream primer, *Eco*RI site	pTA1170
PEecorI F	GCCCGAATTCCGTCTGATTG	Δ*rpa1 operon* external downstream primer, *Eco*RI site	pTA1189
Rpa1CR US	TACTACGTCTAGACGGACCTGTTCG	Δ*rpa1 operon* external upstream primer, *Xba*I site	pTA1189
RPEndeI R DS	CTACCGGAACATATGACTCGGGTCG	Δ*rpa1 operon* internal downstream primer, *Nde*I site	pTA1189
Rpa1ndeI F2	GTTGGACCCATATGTCGAACGACG	Δ*rpa1 operon* internal upstream primer, *Nde*I site	pTA1189
RPAP11SphI US	GCGATTTCCCGCATGCCGACGACCG	Δ*rpap1* internal upstream primer, *Sph*I site	pTA1217
RPAP11 kpnI us	CCGCGAGTGGTACCGCAAGCCCG	Δ*rpap1* external upstream primer, *Kpn*I site	pTA1217
Rpa3BspHI F	AGGTAGATCATGACTGATTTGC	*rpa3* forward primer, *Bsp*HI site	pTA1218
Rpa3 RAseI	CGAGTGGGGAATTCGTTGGAATTAATTTACATC	*rpa3* reverse primer, *Ase*I site	pTA1218
Rpa1F *Nco*I	CCCGACTCCATGGAACTCGACC	*rpa1* forward primer, *Nco*I site	pTA1222
Rpa1AseI/*Eco*RI	CGGCGGCGAATTCGCGGTAGGCGATTAATCGCGTGC pTA1327	*rpa1* reverse primer, *Ase*I and *Eco*RI sites	pTA1222
RPAP1F *Bsp*HI	GGTGCGCTCATGAGCGCCTCG	*rpap1* forward primer, *Bsp*HI site	pTA1223
RPAP1BamHI	CGTTCGGGGGATCCGCGCCTGC pTA1326	*rpap1* reverse primer, *Bam*HI site	pTA1223
RPAP3BspHI F	GTCGATGTTCATGAGTTCCAACG	*rpap3* forward primer, *Bsp*HI site	pTA1224
RPAP3EcoRI R	CGGTCGGAATTCAGGCCGAC pTA1280	*rpap3* reverse primer, *Eco*RI site	pTA1224
HsaCdc48F	GTTCTTGGCATATGACCGAGGCTCTC	Forward primer for *Hsa-cdc48d*, *Nde*I site	pTA1240, Probe **Figure 5B**
HsaCdc48R	CTGACAGATCTCGCAGTCACAGC	Reverse primer for *Hsa-cdc48d*, *Bg*III site	pTA1240, Probe **Figure 5B**
Rpa3BstEII	GATGCGCGGTGACCTCGTGG	*rpap3* forward primer, native *Bst*EII site	pTA1280
Rpa3NdeI	CGAGGTAGCATATGACTGATTTGCG	*rpa3* forward primer, *Nde*I site	pTA1281
RPAP3 gitF	CTCCCAATGGGTACCAAGGTGGAGGC	Δ*rpap3* internal upstream primer, *Nde*I site	pTA1282
RPAP3 gitR	TCGTTGGACATATGTTACATCGACCTCGC	Δ*rpap3* external upstream primer, *Kpn*I site	pTA1282
RPAP3 F DS	CTCGCTGAATTCGGTGGGTGC	Δ*rpap3* external downstream primer, *Eco*RI site	pTA1282
RPAP3 R DS	CTGAGCGCATATGCGGGCGTCTCG	Δ*rpap3* internal downstream primer, *Nde*I site	pTA1282
cdc48dUF	ACGGGTACCCACGTTGCTGG	*Hvo-cdc48d* external upstream primer, *Kpn*I site	pTA1294
cdc48dDR	GCCGAATTCGAGCCGAGGTGG	*Hvo-cdc48d* external downstream primer, *Eco*RI site	pTA1294
cdc48d-CtrR	CGGCGCGCTAGCCGGACCGGTTACGC	Internal reverse primer to generate C-terminally truncated *Hvo-cdc48d*, *Nhe*I site at *cdc48d* stop codon	pTA1294
cdc48d-CtrF	CTGTGGTGCTAGCCGTCGTCCGACCCCG	Internal forward primer to generate C-terminal truncated *Hvo-cdc48d*, *Nhe*I site at *cdc48d* stop codon	pTA1294
cdc48dSeqF	GGAAAAAGGGGCAGATGGTG	Forward primer to downstream flanking region of *Hvo-cdc48d*	PCR **Figure 5C**
cdc48dHvSeqR	CGACGACATCTCGCTGATTCG	Reverse primer to *Hvo-cdc48d* gene	PCR **Figure 5C**
cdc48dHsalSeqR	GGTCAACACGCTGCTGAAGTCC	Reverse primer to *Hsa-cdc48d* gene	PCR **Figure 5C**
Rpa1BstEII	CCGGCACGGTGACCGCCATCC	*rpap1* forward primer, native *Bst*EII site	pTA1326
Rpa1NdeI	CCCGACCATATGGAACTCGACC	*rpa1* forward primer, *Nde*I site	pTA1327

genomic deletions of *rpa1* and *rpa3* were generated using the counter selective pop-in/pop-out method (Allers et al., 2004). To generate the deletion constructs by PCR, *rpa1* and *rpa3* operons were first isolated from wild-type (WT) *H. volcanii* using native *Bsp*EI and *Eco*RI/*Not*I restriction sites, respectively, to generate genomic libraries. These were then screened for the presence of the *rpa1* and *rpa3* operons, individually, using colony hybridization. The isolated plasmids, pTA937 (*rpa1* operon) and pTA884 (*rpa3* operon) were confirmed by DNA sequencing. Deletion constructs for *rpa1* and *rpa3* were designed to avoid polar effects on the expression of the downstream *rpap* genes by maintaining the reading frame. Genomic deletions of both *rpa1* and *rpa3* (*trpA*-marked) were successful, generating strains H1217 and H1244, respectively (**Figures 2** and **3**, respectively). The ability to delete both *rpa1* and *rpa3* with relative ease, but not *rpa2*, indicates that the cellular requirement for each RPA is not equal, making it unlikely that they function collectively.

Both eukaryotic and bacterial SSB are involved in DNA repair. To examine if *H. volcanii* RPA1 and RPA3 function in DNA repair, the effects of DNA damage on cell survival of H1217 and H1244 were examined. UV irradiation results in the formation of cyclobutane pyrimidine dimers and 6-4 pyrimidine-pyrimidone dimer photoproducts, as well as ssDNA nicks that indirectly generate double-stranded DNA breaks (DSBs). The latter require repair by homologous recombination (HR) or single-strand DNA annealing (Fousteri and Mullenders, 2008; Rouillon and White, 2011). MMC is a chemotherapeutic agent that reacts with DNA generating covalent interstrand cross-links, requiring removal by nucleotide excision repair (NER) and HR (Tomasz et al., 1987). The Δ*rpa1* mutant H1217 was no more sensitive than the WT to UV and MMC-induced DNA damage, however the Δ*rpa3* mutant H1244 exhibited moderate sensitivity to both UV and MMC-induced DNA damage (**Figure 4**).

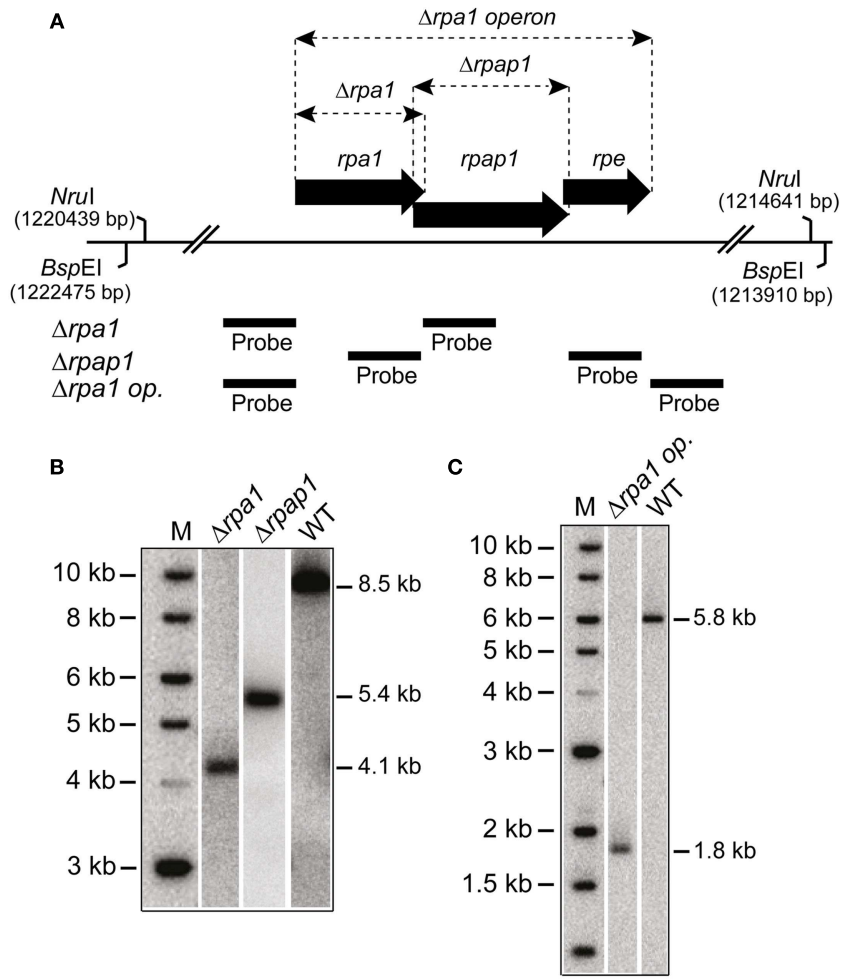

FIGURE 2 | (A) Map of *rpa1* operon indicating location of Δ*rpa1*, Δ*rpap1*, and Δ*rpa1* operon deletions, as well as the *Bsp*EI and *Nru*I sites, and probes used to verify the deletions. (**B**) Southern blot of genomic DNA cut with *Bsp*EI and probed with flanking regions of *rpa1* and *rpap1*, as shown in **(A)**, to indicate deletion of *rpa1* and *rpap1*, respectively. **(C)** Southern blot of genomic DNA cut with *Nru*I and probed with flanking regions of *rpa1* operon (*rpa1 op.*), as shown in **(A)**, to indicate deletion of the *rpa1* operon.

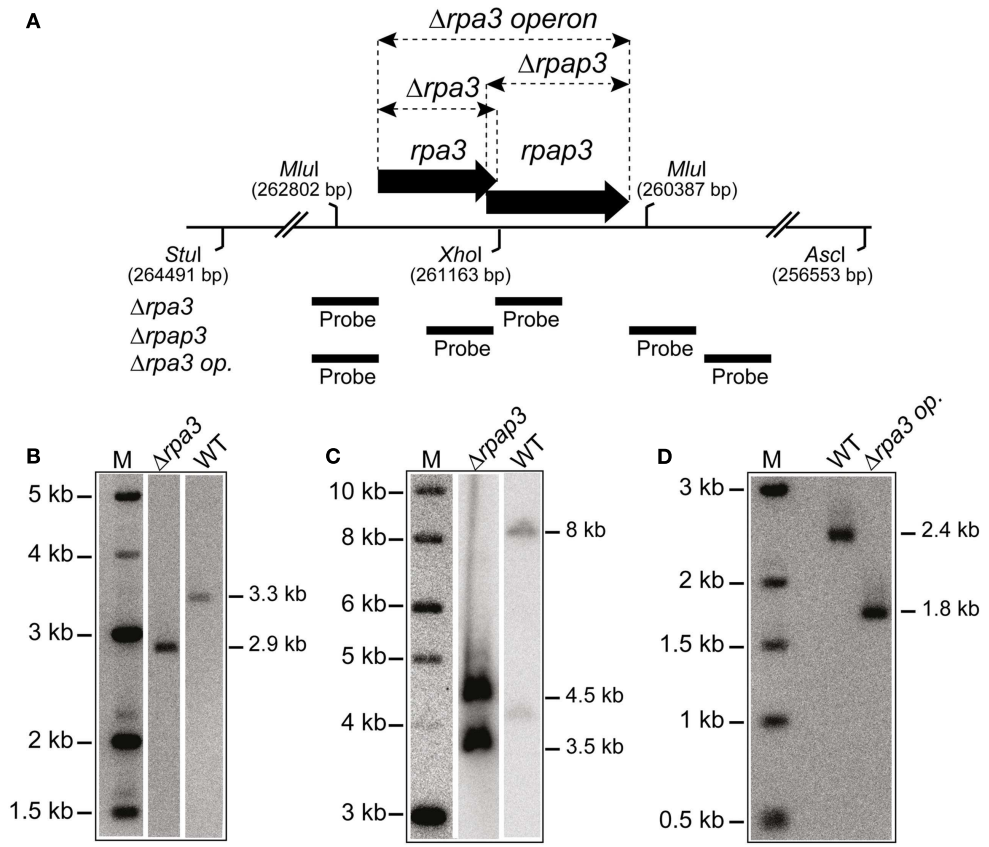

FIGURE 3 | (A) Map of *rpa3* operon indicating location of Δ*rpa3*, Δ*rpap3*, and Δ*rpa3* operon deletions, as well as the *Asc*I, *Mlu*I, *Stu*I, and *Xho*I sites and probes used to verify the deletions. **(B)** Southern blot of genomic DNA cut with *Stu*I and *Xho*I, and probed with flanking regions of *rpa3*, as shown in **Figure 2A**, to indicate deletion of *rpa3*. **(C)** Southern blot of genomic DNA cut with *Asc*I and *Stu*I, and probed with flanking regions of *rpap3*, as shown in **Figure 2A**, to indicate deletion of the *rpap3*. **(D)** Southern blot of genomic DNA cut with *Mlu*I and probed with flanking regions of *rpa3* operon (*rpa3 op.*), as shown in **Figure 2A**, to indicate deletion of the *rpa3* operon.

RPAP3 BUT NOT RPAP1 FUNCTIONS IN DNA REPAIR

Analysis of predicted protein domains indicates that RPA1 and RPA3 both possess zinc finger domains, and that RPA1 has three OB-folds compared to the single OB-fold present in RPA3 (**Figure 1**). Both COG3390 RPAPs RPAP1 and RPAP3 possess a single OB-fold suggesting a possible role in DNA binding. The RPA1 phosphoesterase (RPE) has a calcineurin-like phosphoesterase domain, and was not investigated individually. However, our results and those of Skowyra and MacNeill (2012) show that *rpe* is a non-essential gene.

To study the roles of RPAP1 and RPAP3 in DNA repair, Δ*rpap1* (H1216) and Δ*rpap3* (H1410) mutants were generated, both using *trpA*-marked deletion constructs (**Figures 2** and **3**, respectively). As with Δ*rpa1* strain H1217, the Δ*rpap1* mutant H1216 showed no increased sensitivity to UV irradiation or to MMC-induced DNA damage. However, the Δ*rpap3* deletion mutant H1410 was hypersensitive to both types of DNA damage, and the level of sensitivity was similar to that exhibited by the Δ*rpa3* mutant H1244.

We examined whether the absence of both RPA and RPAP results in a synergistic deficiency in DNA repair. Genomic deletions of the *rpa1* and *rpa3* operons were generated in strains H1246 and H1260, respectively, with only the latter being a *trpA*-marked deletion (**Figures 2** and **3**, respectively); deletions of the *rpa1* and *rpa3* operons have previously been reported by Skowyra and MacNeill (2012). The Δ*rpa1* operon mutant showed no increased sensitivity to UV irradiation or to MMC-induced DNA damage. However the Δ*rpa3* operon deletion mutant was hypersensitive to both types of DNA damage, and the level of sensitivity was similar to that exhibited by the single Δ*rpa3* and Δ*rpap3* mutants H1244 and H1410, respectively (**Figure 4**). This result suggests that RPA3 and RPAP3 function in the same pathway(s) of DNA repair.

REDUNDANCY BETWEEN RPA1 AND RPA3 OPERONS

In order to test for redundancy between the two RPAs, an attempt was made to generate a double Δ*rpa1* operon Δ*rpa3* operon deletion. This involved constructing the strain H1282, which contained the pop-in of a *trpA*-marked Δ*rpa3* operon construct (pTA1207) in an unmarked Δ*rpa1* operon background (H1246). An episomal plasmid (pTA1265), marked with *pyr*E2 and providing in *trans* expression of the *rpa1* operon was used for complementation during the pop-out step (note that this episomal plasmid is lost during counter-selection with 5-FOA). Neither of the two pop-outs generated from this strain (H1390) yielded the desired Δ*rpa1* operon

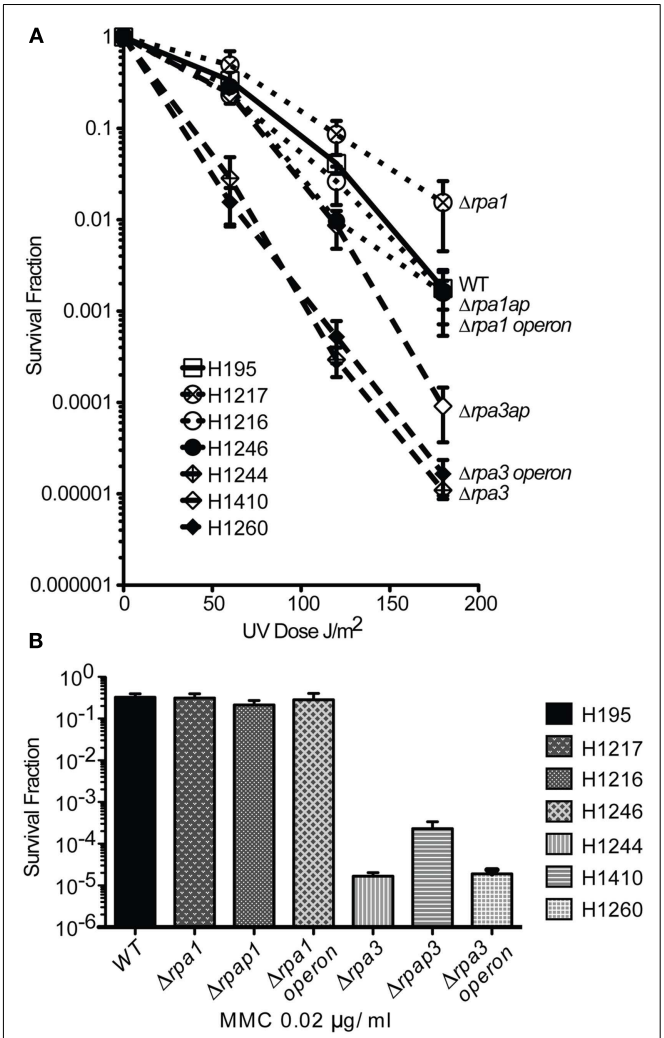

FIGURE 4 | (A) Wild-type (WT), *rpa1*, *rpap1*, *rpa1* operon, *rpa3*, *rpap3*, *rpa3* operon (H195, H1217, H1216, H1246, H1244, H1410, and H1260, respectively), were plated out and exposed to ultraviolet (UV) radiation. The average and standard error (SE) of three experiments are shown. **(B)** The strains shown in **(A)** were plated out and exposed to mitomycin C (MMC). The average and SE of three experiments are shown.

Δ*rpa3* operon mutant (see **Figure A1** in Appendix). This indicates that the cell requires either RPA1 or RPA3 (and/or their respective RPAPs) for survival.

Next we attempted to generate Δ*rpa1* Δ*rpap3* and Δ*rpa3* Δ*rpap1* deletion mutants. This would test whether the RPAPs can complement each other, or whether they are instead specific for their respective RPAs. The *trpA*-marked Δ*rpap3* construct (pTA1284) was used in an unmarked Δ*rpa1* background (H1280), and the *trpA*-marked Δ*rpa3* construct (pTA1207) was used in an unmarked Δ*rpap1* background (H1281). In both cases two pop-outs were generated but none proved to be the desired deletions (see **Figure 1** in Appendix). This suggests that the putative RPA:RPAP complex is dependent upon specific RPA:RPAP interactions for functionality.

CONSTRUCTION OF PROTEIN OVEREXPRESSION STRAIN WITH C-TERMINAL TRUNCATION OF CDC48D

In a previous publication (Allers et al., 2010), we constructed a strain of *H. volcanii* where the histidine-rich *pitA* gene is replaced by the ortholog from *N. pharaonis*. The latter protein lacks the histidine-rich linker region found in *H. volcanii* PitA and does not co-purify with His-tagged recombinant proteins. The absence of Hvo-PitA revealed an additional co-purifying protein, which we identified as Cdc48d (HVO_1907) and features a histidine-rich C-terminus (**Figure 5A**). We were unable to delete *cdc48d*, indicating that this gene is essential (Allers et al., 2010). The presence of this contaminating protein was problematic for purification of His-tagged RPA1 and RPAP1, due to similar molecular weights (Cdc48d, 53 kDa; RPA1, 46 kDa; RPAP1, 65 kDa).

All orthologs of Cdc48d from haloarchaea feature a histidine-rich C-terminus, however Cdc48d from *Haloarcula marismortui* and *H. salinarum* have only three and four histidines, respectively, compared to six in *H. volcanii* (**Figure 5A**). Therefore, we replaced the *H. volcanii cdc48d* gene in H1209 (Allers et al., 2010) with orthologous genes from *H. marismortui* and *H. salinarum*, generating *H. volcanii* strains H1405 and H1333, respectively. Unfortunately these strains grew poorly and were not suitable for recombinant protein overexpression. Instead, we generated a truncated allele of *H. volcanii cdc48d*, encoding a Cdc48d protein lacking the histidine-rich C-terminus (Cdc48d-Ct; **Figure 5A**). The *cdc48d-Ct* allele was used to replace the *H. salinarum cdc48d* gene in *H. volcanii* H1333, generating H1424 (**Figures 5B,C**). This strain exhibits normal cell growth and the Cdc48d-Ct protein no longer co-purifies with His-tagged recombinant proteins (**Figure 5D**). A number of minor histidine-rich contaminants are now apparent, which have been identified by mass spectrometry.

DIRECT RPAP INTERACTION WITH RESPECTIVE RPA

The genetic analysis of *rpa1* and *rpa3* and their respective *rpap* genes indicates not only that RPA3 and RPAP3 function in the same DNA repair pathway(s), but also that they function together as a specific RPA:RPAP complex. To establish whether this is achieved via a direct RPA:RPAP interaction, affinity pull-downs were employed (Allers et al., 2010). The *rpa1* and *rpa3* operons were cloned under control of the tryptophanase promoter in plasmid pTA963, where either the RPA or the RPAP was tagged with a hexahistidine tag.

Histidine-tagged RPA1 and RPA3 pulled down their respective RPAPs, and histidine-tagged RPAP1 and RPAP3 pulled down their respective RPAs (**Figure 6**). However, histidine-tagged RPA1 did not pull down RPAP3, and vice versa. This confirms that the RPAs interact specifically with their respective RPAPs, supporting our conclusions based on the failure to generate Δ*rpa1* Δ*rpap3* and Δ*rpa3* Δ*rpap1* deletion mutants. Neither RPA1 nor RPA3 pulled down RPA2, and histidine-tagged RPA2 did not pull down RPA1 or 3, or either of the RPAPs (data not shown). This supports the suggestion that the three RPAs of *H. volcanii* do not form a heterotrimer as observed in eukaryotes and *P. furiosus*, but instead form three separate ssDNA-binding factors.

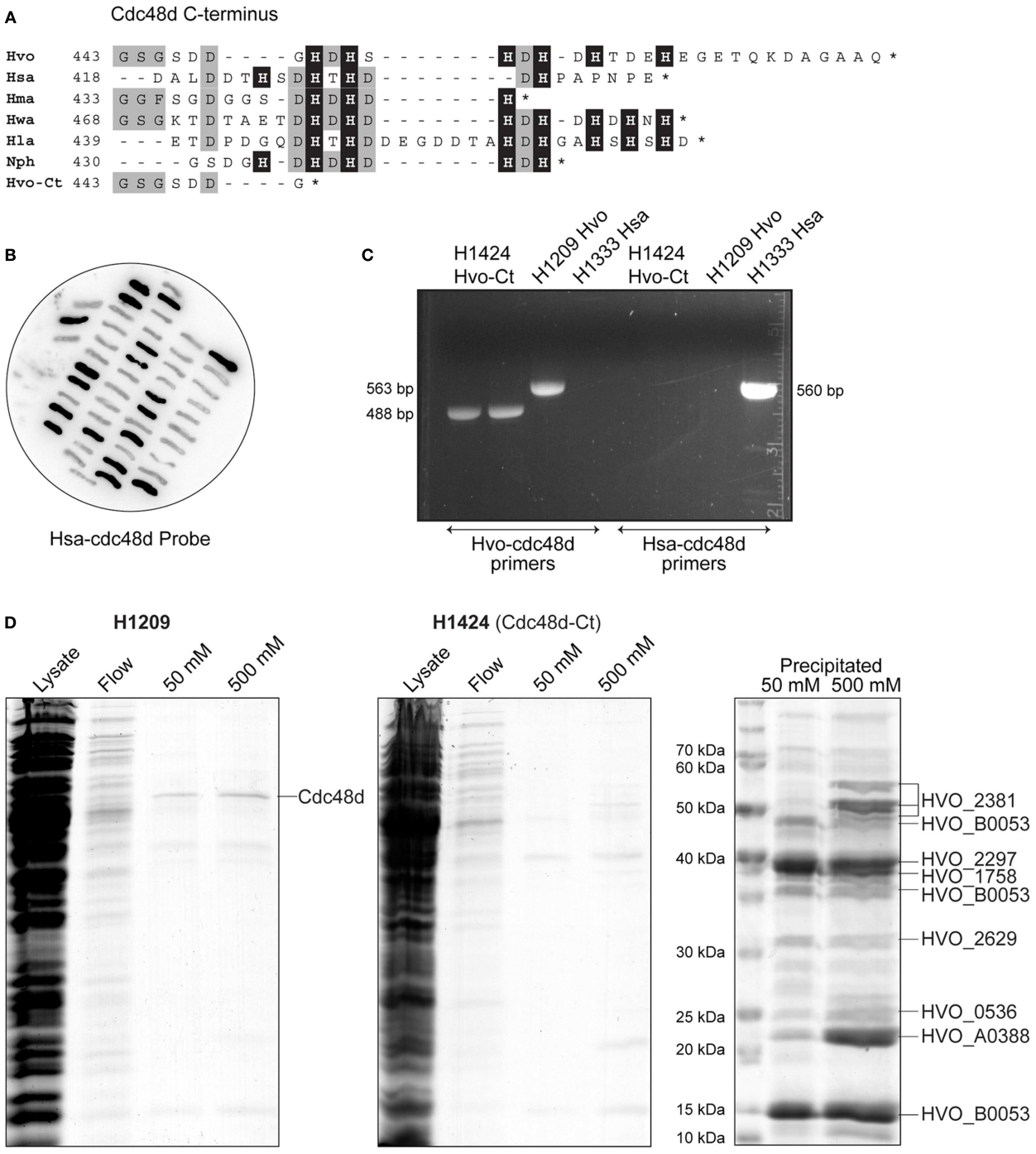

FIGURE 5 | (A) Protein sequence alignment of C-terminus of Cdc48d from selected species of haloarchaea (Hvo, *H. volcanii*; Hsa, *Halobacterium salinarum*; Hma, *Haloarcula marismortui*; Hwa, *Haloquadratum walsbyi*; Hla, *Halorubrum lacusprofundi*; Nph, *N. pharaonis*; Hvo-Ct, *H. volcanii* C-terminal truncation Cdc48d-Ct). Histidine residues are indicated by a black background. **(B)** Colony hybridization of 5-FOA-resistant clones of *H. volcanii* H1333, after pop-in/pop-out gene replacement with pTA1294. *H. salinarum cdc48d* sequences (*Hsa-cdc48d*) were used as a probe, clones failing to hybridize therefore carry the truncated *H. volcanii cdc48d-Ct* allele present in pTA1294. **(C)** Verification of truncated *cdc48d-Ct* allele in H1424 by PCR (488 bp product), with primers specific to either *H. volcanii* or *H. salinarum* genes. H1209 genomic DNA was used as a control for wild-type *H. volcanii cdc48d* (563 bp product), and H1333 was used as a control for *H. salinarum cdc48d* (560 bp product). **(D)** *H. volcanii* strains H1209 and H1424 containing empty vector pTA963 (Allers et al., 2010) were used in mock protein overexpression. Histidine-rich cellular proteins were purified from the soluble fraction (lysate) by affinity chromatography on a Ni^{2+} chelating column, samples were taken from the flow-through (flow) and bound proteins were eluted using 50 and 500 mM imidazole. Precipitation using trichloroacetic acid and deoxycholate was used to enhance visualization and identification of the eluted proteins by mass spectrometry. Cdc48d (HVO_1907) eluted from cell extracts of H1209 but not from H1424 (*cdc48d-Ct*).

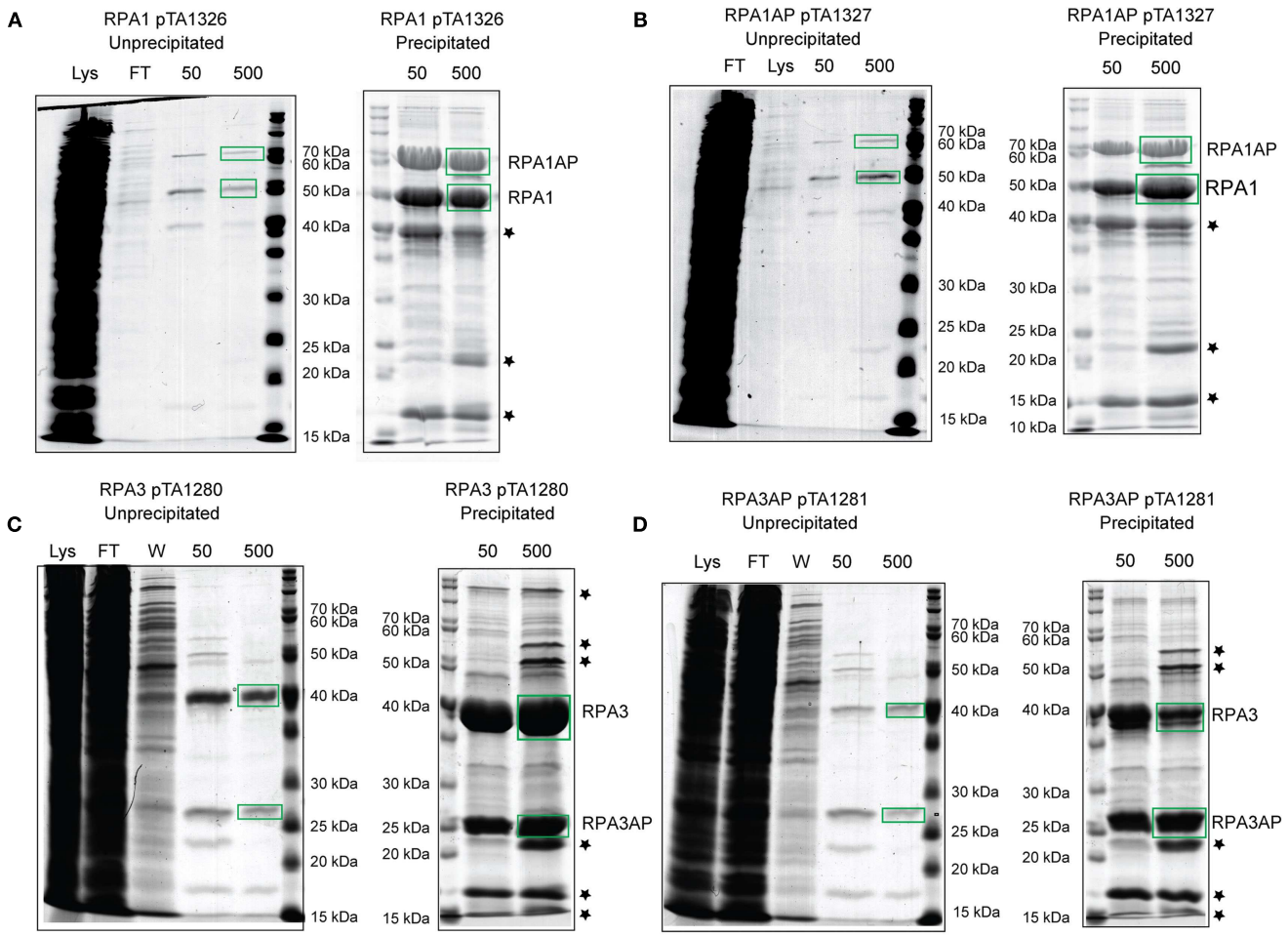

FIGURE 6 | *H. volcanii* strains containing (A) histidine-tagged RPA1 (H1482), (B) histidine-tagged RPAP1 (H1483), (C) histidine-tagged RPA3 (H1480), and (D) histidine-tagged RPAP3 (H1481) were used in protein overexpression. The histidine-tagged recombinant proteins were purified from the soluble fraction (lysate) by affinity chromatography on a Ni^{2+} chelating column, samples were taken from the flow-through (FT) and bound proteins were eluted using 50 and 500 mM imidazole. Precipitation using trichloroacetic acid and deoxycholate was used to enhance visualization and identification of the eluted proteins by mass spectrometry. Stars denote contaminants shown in **Figure 5D**.

DISCUSSION

There is a unifying theme in archaea of a great variety in the number and type of proteins involved in DNA replication, and repair, whose counterparts in eukaryotes are much more uniform. This has been shown to be the case for RPA, where eukaryotes possess three subunits that all form unified clades in a phylogenetic analysis, but in archaea the number and structure of subunits varies widely. Some euryarchaea possess differing numbers of RPA subunits and some possess differing numbers of RPAs and RPAPs. Crenarchaea also possess varying numbers of SSB, however in both euryarchaea and crenarchaea none of the RPAs, RPAPs, or SSBs fall into unified clades. Again this is seen in the case of MCM, where eukaryotes possess six MCM subunits that each form unified clades, but in archaea there is a vast range in the number of MCM subunits, differing between individual species, and none of which fall into uniform clades (Chia et al., 2010). Characterizing the RPA-RPAP complexes of *H. volcanii* will shed light on how the RPAs and RPAPs function together in binding and stabilizing ssDNA. This in turn will provide insight for other RPAs and RPAPs in archaea, but also offer reasoning behind the driving force of such non-uniform evolution of archaea.

The genetic and biochemical analysis presented here indicates the three RPAs of *H. volcanii* do not form a heterotrimeric complex as in *P. furiosus* and eukaryotes. Instead, RPA1 and RPA3 form complexes with their respective RPAPs. Unlike *rpa2*, both *rpa1* and *rpa3* genomic deletions were generated with relative ease, showing that the latter are not essential for cell survival and supporting the hypothesis that the three RPAs do not form a heterotrimeric complex.

The ease at which the *rpa1*, *rpap1*, and *rpa1* operon deletion mutants were made, coupled with a lack DNA damage sensitivity, signifies the *rpa1* operon does not play a major role in DNA replication or repair. The moderate DNA damage sensitivity shown by the individual *rpa3*, *rpap3*, and the *rpa3* operon mutants indicates that the efficient repair of UV and MMC-induced DNA damage requires the products of the *rpa3* operon but not the

rpa1 operon. However, it proved impossible to generate a double Δ*rpa1* operon Δ*rpa3* operon deletion, showing that cellular growth requires either RPA1 or RPA3.

Both single Δ*rpa3* and Δ*rpap3* mutants showed a similar DNA damage sensitivity to each other, and to the *rpa3* operon mutant, providing genetic evidence that RPA3 and RPAP3 act in the same DNA repair pathway. Furthermore, we were unable to generate Δ*rpa1* Δ*rpap3* and Δ*rpa3* Δ*rpap1* deletion mutants, indicating that RPAP1 could not substitute for RPAP3 (and vice versa), and suggesting that the RPA3 interacts specifically with RPAP3 (and likewise for RPA1 and RPAP1). However it is unclear what role the associated proteins play, since the presence of an OB-fold does not necessarily indicate direct ssDNA binding. Instead, the RPAPs may provide a platform for protein:protein interactions. This is seen in eukaryotes, where the RPA 14 kDa subunit possesses a single OB-fold, this subunit is essential for formation of the RPA heterotrimer by facilitating protein:protein interactions (Fanning et al., 2006).

The co-purification of histidine-tagged RPA1 and RPA3 with their respective untagged RPAPs (and vice versa) supports our hypothesis that *H. volcanii* RPA1 and RPA3 form complexes with their respective RPAPs. This observation, and the differing outcomes of *rpa1*, *rpa2*, and *rpa3* deletions, indicates that the three RPAs of *H. volcanii* do not function as a heterotrimer. Similar results have been obtained in *M. acetivorans*, where the three RPAs are able to bind ssDNA individually, in addition to stimulating primer extension by *M. acetivorans* DNA polymerase BI *in vitro*. (Robbins et al., 2004).

This study has shown genetically and biochemically that RPAPs interact with RPAs, and that this interaction is RPA-specific. This is the first report investigating the function of the archaeal COG3390 RPA-associated proteins (RPAPs), thus providing an important insight of the structure and function of *H. volcanii* single-strand DNA-binding proteins.

AUTHOR CONTRIBUTIONS

Amy Stroud and Thorsten Allers wrote the paper; Amy Stroud and Thorsten Allers designed the experiments; Amy Stroud and Thorsten Allers performed the microbiological and biochemical experiments; Susan Liddell carried out the mass spectrometry; Amy Stroud, Susan Liddell, and Thorsten Allers analyzed the data.

ACKNOWLEDGMENTS

We are grateful to the BBSRC for a PhD studentship awarded to Amy Stroud and the Royal Society for a University Research Fellowship awarded to Thorsten Allers. We thank Kayleigh Wardell for help with strain construction, and Ed Bolt, Geoff Briggs, and Karen Bunting for their advice.

REFERENCES

Alberts, B. M., and Frey, L. (1970). T4 bacteriophage gene 32: a structural protein in the replication and recombination of DNA. *Nature* 227, 1313–1318.

Allers, T., Barak, S., Liddell, S., Wardell, K., and Mevarech, M. (2010). Improved strains and plasmid vectors for conditional overexpression of His-tagged proteins in *Haloferax volcanii*. *Appl. Environ. Microbiol.* 76, 1759–1769.

Allers, T., Ngo, H. P., Mevarech, M., and Lloyd, R. G. (2004). Development of additional selectable markers for the halophilic archaeon *Haloferax volcanii* based on the leuB and trpA genes. *Appl. Environ. Microbiol.* 70, 943–953.

Berthon, J., Cortez, D., and Forterre, P. (2008). Genomic context analysis in Archaea suggests previously unrecognized links between DNA replication and translation. *Genome Biol.* 9, R71.

Bochkarev, A., and Bochkareva, E. (2004). From RPA to BRCA2: lessons from single-stranded DNA binding by the OB-fold. *Curr. Opin. Struct. Biol.* 14, 36–42.

Brill, S. J., and Stillman, B. (1991). Replication factor-A from *Saccharomyces cerevisiae* is encoded by three essential genes coordinately expressed at S phase. *Genes Dev.* 5, 1589–1600.

Chia, N., Cann, I., and Olsen, G. J. (2010). Evolution of DNA replication protein complexes in eukaryotes and Archaea. *PLoS ONE* 5, e10866. doi:10.1371/journal.pone.0010866

Coverley, D., Kenny, M. K., Lane, D. P., and Wood, R. D. (1992). A role for the human single-stranded DNA binding protein HSSB/RPA in an early stage of nucleotide excision repair. *Nucleic Acids Res.* 20, 3873–3880.

Coverley, D., Kenny, M. K., Munn, M., Rupp, W. D., Lane, D. P., and Wood, R. D. (1991). Requirement for the replication protein SSB in human DNA excision repair. *Nature* 349, 538–541.

Cubeddu, L., and White, M. F. (2005). DNA damage detection by an archaeal single-stranded DNA-binding protein. *J. Mol. Biol.* 353, 507–516.

Delmas, S., Shunburne, L., Ngo, H. P., and Allers, T. (2009). Mre11-Rad50 promotes rapid repair of DNA damage in the polyploid archaeon *Haloferax volcanii* by restraining homologous recombination. *PLoS Genet.* 5, e1000552. doi:10.1371/journal.pgen.1000552

Fanning, E., Klimovich, V., and Nager, A. R. (2006). A dynamic model for replication protein A (RPA) function in DNA processing pathways. *Nucleic Acids Res.* 34, 4126–4137.

Fousteri, M., and Mullenders, L. H. (2008). Transcription-coupled nucleotide excision repair in mammalian cells: molecular mechanisms and biological effects. *Cell Res.* 18, 73–84.

Guy, C. P., Haldenby, S., Brindley, A., Walsh, D. A., Briggs, G. S., Warren, M. J., Allers, T., and Bolt, E. L. (2006). Interactions of RadB, a DNA repair protein in Archaea, with DNA and ATP. *J. Mol. Biol.* 358, 46–56.

Hartman, A. L., Norais, C., Badger, J. H., Delmas, S., Haldenby, S., Madupu, R., Robinson, J., Khouri, H., Ren, Q., Lowe, T. M., Maupin-Furlow, J., Pohlschroder, M., Daniels, C., Pfeiffer, F., Allers, T., and Eisen, J. A. (2010). The complete genome sequence of *Haloferax volcanii* DS2, a model archaeon. *PLoS ONE* 5, e9605. doi:10.1371/journal.pone.0009605

Haseltine, C. A., and Kowalczykowski, S. C. (2002). A distinctive single-strand DNA-binding protein from the archaeon *Sulfolobus solfataricus*. *Mol. Microbiol.* 43, 1505–1515.

Heyer, W. D., Rao, M. R., Erdile, L. F., Kelly, T. J., and Kolodner, R. D. (1990). An essential *Saccharomyces cerevisiae* single-stranded DNA binding protein is homologous to the large subunit of human RP-A. *EMBO J.* 9, 2321–2329.

Kenny, M. K., Lee, S. H., and Hurwitz, J. (1989). Multiple functions of human single-stranded-DNA binding protein in simian virus 40 DNA replication: single-strand stabilization and stimulation of DNA polymerases alpha and delta. *Proc. Natl. Acad. Sci. U.S.A.* 86, 9757–9761.

Kerr, I. D., Wadsworth, R. I., Cubeddu, L., Blankenfeldt, W., Naismith, J. H., and White, M. F. (2003). Insights into ssDNA recognition by the OB fold from a structural and thermodynamic study of *Sulfolobus* SSB protein. *EMBO J.* 22, 2561–2570.

Kim, C., Snyder, R. O., and Wold, M. S. (1992). Binding properties of replication protein A from human and yeast cells. *Mol. Cell. Biol.* 12, 3050–3059.

Komori, K., and Ishino, Y. (2001). Replication protein A in *Pyrococcus furiosus* is involved in homologous DNA recombination. *J. Biol. Chem.* 276, 25654–25660.

Lestini, R., Duan, Z., and Allers, T. (2010). The archaeal Xpf/Mus81/FANCM homolog Hef and the Holliday junction resolvase Hjc define alternative pathways that are essential for cell viability in *Haloferax volcanii*. *DNA Repair (Amst.)* 9, 994–1002.

Lin, Y., Lin, L. J., Sriratana, P., Coleman, K., Ha, T., Spies, M., and Cann, I. K. (2008). Engineering of functional replication protein a homologs based on insights into the evolution of oligonucleotide/oligosaccharide-binding folds. *J. Bacteriol.* 190, 5766–5780.

Lu, D., and Keck, J. L. (2008). Structural basis of *Escherichia coli* single-stranded DNA-binding protein

stimulation of exonuclease I. *Proc. Natl. Acad. Sci. U.S.A.* 105, 9169–9174.

Lu, D., Windsor, M. A., Gellman, S. H., and Keck, J. L. (2009). Peptide inhibitors identify roles for SSB C-terminal residues in SSB/exonuclease I complex formation. *Biochemistry* 48, 6764–6771.

Moore, S. P., Erdile, L., Kelly, T., and Fishel, R. (1991). The human homologous pairing protein HPP-1 is specifically stimulated by the cognate single-stranded binding protein hRP-A. *Proc. Natl. Acad. Sci. U.S.A.* 88, 9067–9071.

Mullakhanbhai, M. F., and Larsen, H. (1975). *Halobacterium volcanii* spec. nov., a Dead Sea halobacterium with a moderate salt requirement. *Arch. Microbiol.* 104, 207–214.

Robbins, J. B., McKinney, M. C., Guzman, C. E., Sriratana, B., Fitz-Gibbon, S., Ha, T., and Cann, I. K. (2005). The euryarchaeota, nature's medium for engineering of single-stranded DNA-binding proteins. *J. Biol. Chem.* 280, 15325–15339.

Robbins, J. B., Murphy, M. C., White, B. A., Mackie, R. I., Ha, T., and Cann, I. K. (2004). Functional analysis of multiple single-stranded DNA-binding proteins from *Methanosarcina acetivorans* and their effects on DNA synthesis by DNA polymerase BI. *J. Biol. Chem.* 279, 6315–6326.

Rolfsmeier, M. L., and Haseltine, C. A. (2010). The single-stranded DNA binding protein of *Sulfolobus solfataricus* acts in the presynaptic step of homologous recombination. *J. Mol. Biol.* 397, 31–45.

Rouillon, C., and White, M. F. (2011). The evolution and mechanisms of nucleotide excision repair proteins. *Res. Microbiol.* 162, 19–26.

Sambrook, J., and Russell, D. W. (2001). *Molecular Cloning: A Laboratory Manual*. Cold Spring Harbor, NY: Cold Spring Harbor Laboratory Press.

Skowyra, A., and MacNeill, S. A. (2012). Identification of essential and non-essential single-stranded DNA-binding proteins in a model archaeal organism. *Nucleic Acids Res.* 40, 1077–1090.

Tomasz, M., Lipman, R., Chowdary, D., Pawlak, J., Verdine, G. L., and Nakanishi, K. (1987). Isolation and structure of a covalent cross-link adduct between mitomycin C and DNA. *Science* 235, 1204–1208.

Wobbe, C. R., Weissbach, L., Borowiec, J. A., Dean, F. B., Murakami, Y., Bullock, P., and Hurwitz, J. (1987). Replication of simian virus 40 origin-containing DNA in vitro with purified proteins. *Proc. Natl. Acad. Sci. U.S.A.* 84, 1834–1838.

Wold, M. S. (1997). Replication protein A: a heterotrimeric, single-stranded DNA-binding protein required for eukaryotic DNA metabolism. *Annu. Rev. Biochem.* 66, 61–92.

Wold, M. S., Weinberg, D. H., Virshup, D. M., Li, J. J., and Kelly, T. J. (1989). Identification of cellular proteins required for simian virus 40 DNA replication. *J. Biol. Chem.* 264, 2801–2809.

Conflict of Interest Statement: The authors declare that the research was conducted in the absence of any commercial or financial relationships that could be construed as a potential conflict of interest.

Received: 15 March 2012; accepted: 31 May 2012; published online: 18 June 2012.

Citation: Stroud A, Liddell S and Allers T (2012) Genetic and biochemical identification of a novel single-stranded DNA-binding complex in Haloferax volcanii. Front. Microbio. ***3****:224. doi: 10.3389/fmicb.2012.00224*

This article was submitted to Frontiers in Evolutionary and Genomic Microbiology, a specialty of Frontiers in Microbiology.

APPENDIX

Table A1 | Identification of proteins present in cellular soluble fraction after purification by affinity chromatography on a Ni^{2+} chelating column.

Prot accession	Protein name	HVO_#	Predicted MW	Observed MW	MASCOT score	Number of peptides	% coverage	Peptide sequences
gi[292655491]	RPAP1	1337	64,829	57,781	671	12	18	8
gi[292655492]	RPA1	1338	45,954	36,960	940	15	40	11
gi[292655491]	RPAP1	1337	64,829	62,780	578	10	21	9
gi[292655492]	RPA1	1338	45,954	45,686	808	15	40	12
gi[292654471]	RPAP3	0291	21,979	15,074	435	10	53	7
gi[292654471]	RPAP3	0291	21,979	16,217	484	10	59	8
gi[292654472]	RPA3	0292	34,562	28,262	796	13	43	10
gi[292654472]	RPA3	0292	34,562	31,741	735	13	48	11
gi[292656508]	Hypothetical protein	2381	52,319	55,300/50,200	240	5	11	5
gi[292493992]	Hypothetical protein	B0053	13,897	4,73,600	259	4	33	3
gi[292656425]	Deoxyhypusine synthase	2297	38,616	39,500	451	7	25	4
gi[292655899]	Thioredoxin reductase	1758	36,505	38,000	312	6	21	6
gi[292493992]	Hypothetical protein	B0053	13,897	36,300	208	6	40	4
gi[292656748]	Htr-like protein	2629	30,266	31,700	93	4	17	4
gi[292654704]	Ferritin	0536	19,892	24,900	66	1	6	1
gi[292653937]	Transcriptional regulator	A0388	20,201	22,300	586	15	54	8
gi[292493992]	Hypothetical protein	B0053	13,897	13,500	170	3	33	3

Prot Accession, the database entry, e.g., gi|292655491; predicted MW, predicted molecular weight (Da) of the protein sequence identified by MASCOT; observed MW, molecular weight estimated from migration on SDS-PAGE; MASCOT score, MASCOT score associated with protein identification; number of peptides, no. of peptides associated with protein identification by MASCOT; % coverage, % of the database sequence entry that is covered by the peptides matched to it in the MASCOT data. Peptide sequences, the number of distinct peptide sequences associated with the protein identified by MASCOT.

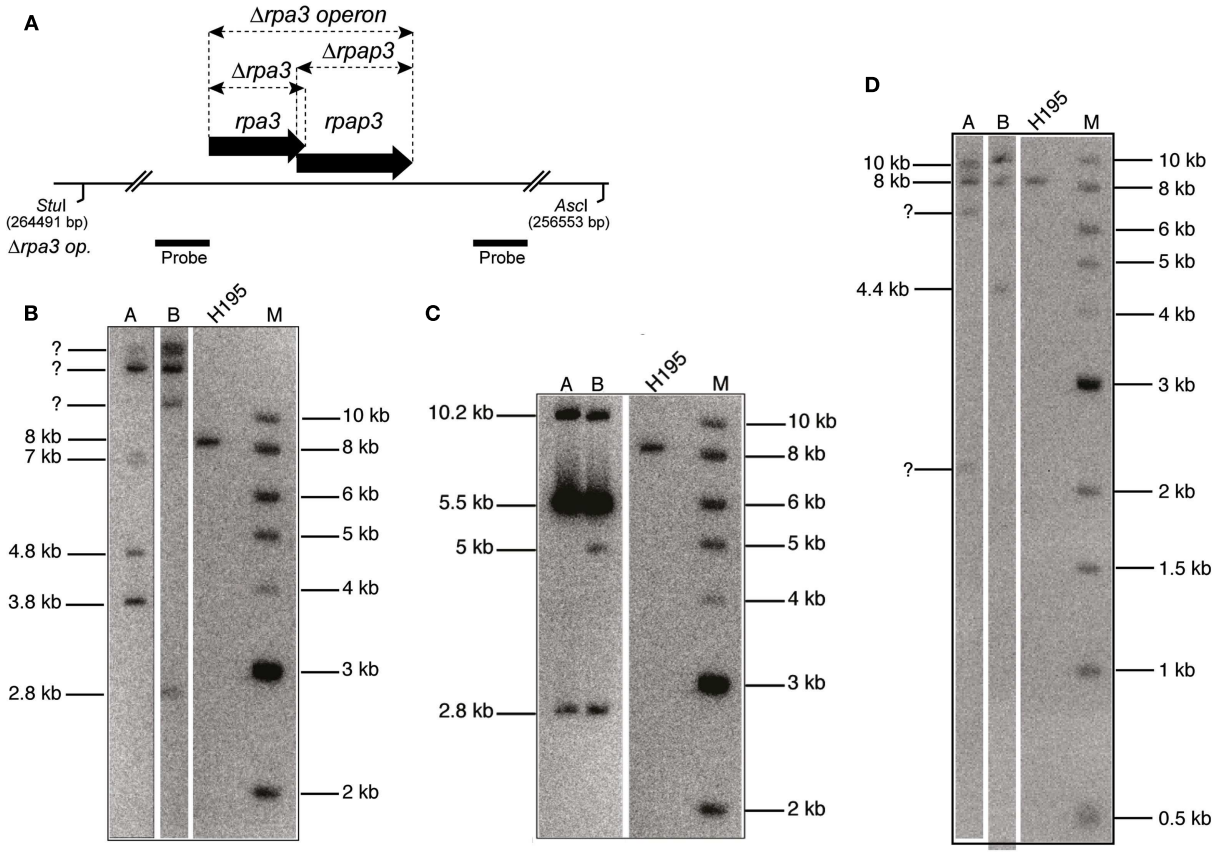

FIGURE A1 | (A) Map of *rpa3* operon indicating location of Δ*rpa3*, Δ*rpap3*, and Δ*rpa3* operon deletions, as well as the *Asc*I and *Stu*I sites and the probe used to verify the deletions. The size of this fragment in the wild-type (H195) is 8 kb. **(B)** Southern blot of genomic DNA cut with *Asc*I and *Stu*I, and probed with flanking regions of *rpa3* operon (*rpa3 op.*), as shown in **(A)**, indicates failure to generate Δ*rpa1* Δ*rpap3* mutant as bands of the expected size for deletion are not seen (3.4 and 4.4 kb). **(C)** Southern blot of genomic DNA cut with *Asc*I and *Stu*I, and probed with flanking regions of *rpa3 op.*, as shown in **(A)**, indicates failure to generate Δ*rpap1* Δ*rpa3* mutant as bands of the expected size for deletion are not seen (2.8 and 5 kb). **(D)** Southern blot of genomic DNA cut with *Asc*I and *Stu*I, and probed with flanking regions of *rpa3 op.*, as shown in **(A)** indicates failure to generate Δ*rpa1* operon Δ*rpa3* operon mutant as bands of the expected size for deletion are not seen (2.8 and 3.4 kb).